

# Reliability of measuring the fat content of the lumbar vertebral marrow and paraspinal muscles using MRI mDIXON-Quant sequence

Yong Zhang\*   
 Zhuang Zhou\*   
 Chao Wang   
 Xiaoguang Cheng   
 Ling Wang   
 Yangyang Duanmu   
 Chenxin Zhang   
 Nicola Veronese   
 Giuseppe Guglielmi 

## PURPOSE

We aimed to assess the reliability of measuring the fat content of the lumbar vertebral marrow and the paraspinal muscles using magnetic resonance imaging (MRI) mDIXON-Quant sequence.

## METHODS

Thirty-one healthy volunteers were included. All participants underwent liver mDIXON-Quant imaging on a 3.0 T Philips MRI scanner by observer A. Within two weeks, observer B repeated the scan. After the examination, each observer independently measured the fat content of the third lumbar vertebra (L3), and the psoas (PS), erector spinae (ES), and multifidus (MF) muscles on central L3 axial images. After two weeks, each observer repeated the same measurements. They were blinded to their previous results. Reliability was estimated by evaluating the repeatability and reproducibility.

## RESULTS

The repeatability of the fat content measurements of L3, PS, ES, and MF was high. The intraclass correlation coefficients of the fat content of L3, PS, ES, and MF were 0.997, 0.984, 0.997, and 0.995 for observer A and 0.948, 0.974, 0.963, and 0.995 for observer B, respectively. The reproducibility of the measurement of the fat content of L3, PS, ES, and MF was high, and the interclass correlation coefficients were 0.984, 0.981, 0.977, and 0.998, respectively.

## CONCLUSION

Using mDIXON-Quant imaging to measure the fat content of the lumbar vertebral marrow and paraspinal muscles shows high reliability and is suitable for use in clinical practice.

From the Department of Radiology (Y.Z., X.C. ✉ xiao65@263.net, L.W., Y.D., C.Z.), Beijing Jishuitan Hospital, Beijing, China; Department of Orthopedic Oncology (Z.Z.), Third Hospital of Hebei Medical University, Shijiazhuang, Hebei, China; Beijing Institute of Traumatology and Orthopedics (C.W.), Beijing, China; Aging Branch (N.V.), National Research Council, Neuroscience Institute, Padova, Italy; Department of Radiology (G.G. ✉ giuseppe.guglielmi@unifg.it) University of Foggia, Foggia, Italy; Department of Radiology (G.G.), Scientific Institute "Casa Sollievo della Sofferenza" Hospital, San Giovanni Rotondo, Foggia, Italy.

\*These authors contributed equally to this work.

Received 18 August 2017; revision requested 3 October 2017; last revision received 14 March 2018; accepted 23 March 2018.

Published online 9 August 2018.

DOI 10.5152/dir.2018.17323

**F**at is stored in adipose and in other tissues, such as the vertebral marrow and skeletal muscle (1–3). An excess infiltration of fat inside the muscle, which also occurs in skeletal muscles, is an important finding associated with several diseases such as impaired glucose tolerance (4), insulin resistance and type II diabetes (5), obesity (6), reduced muscle activity (7), clinical fractures (5), myositis, and probably cancer (8). Many studies have also reported increased fatty infiltration within the paraspinal muscles of patients with low back pain (9) and long-term denervation (10). The fat content within skeletal muscles may be influenced by age and sex (11), training situations (12), inactivity (12), and recently performed exercises (13). The extent of muscle fatty degeneration may be useful for diagnosis and treatment of some diseases. Bone marrow is a complex heterogeneous admixture, consisting of both hematopoietic and fatty marrow. In humans, increased vertebral marrow fat occurs with osteoporosis (14), aging (15), alcoholism (16), starvation (17), prolonged bed rest (18), spinal cord injury (19), cancer metastasis to bone, chemotherapy and radiation therapy (20). Among these diseases, osteoporotic fractures have a very high morbidity and mortality. Lifetime risk of any osteoporotic fracture is very high and lies within the range of 40%–50% for women and 13%–22% for men (21). Bone marrow fat plays an important role in bone loss; the measurement of marrow fat content might be a helpful tool to promote our understanding of osteoporosis. In particular, it could act as a marker for neoplastic bone marrow diseases and bone marrow healing. Therefore, an effective approach for quantitatively evaluating muscle and marrow fat would include accurate detection of disease and accurate grading of disease severity (22), to devel-

You may cite this article as: Zhang Y, Zhou Z, Wang C, et al. Reliability of measuring the fat content of the lumbar vertebral marrow and paraspinal muscles using MRI mDIXON-Quant sequence. *Diagn Interv Radiol* 2018; 24:302-307.

op interventions for reducing the risk of osteoporosis and type-2 diabetes mellitus, and treating myopathy (23).

The fat content of the lumbar vertebral marrow and paraspinal muscles can be quantified by different methods, each with its advantages and drawbacks. Biopsy is an invasive procedure with a substantial degree of sampling error. Ultrasonography (US) is an alternative method for assessing intramuscular adipose tissue, based on echo intensity (24). US assessment for steatosis is usually subjective and significant observer variation can occur (25). The assessment of fat content through computed tomography (CT) is based on the characteristic attenuation of X-rays by different tissues, and lipid infiltration is the most widely accepted reason for decreased attenuation of muscle (2). Magnetic resonance imaging (MRI) appears to be the most objective and sensitive imaging method for the identification and quantification of marrow and muscle steatosis. Unlike US and CT, which assess muscle steatosis by proxy parameters (echogenicity and attenuation, respectively), MRI and magnetic resonance spectroscopy (MRS) can assess the amount of muscle fat content and marrow more directly. In comparison with previous studies (1, 26), MRI techniques possess the advantage of noninvasive tissue characterization *in vivo* for providing information about muscle structure, architecture, and metabolism in a single examination. MRI can be utilized to quantify the actual fat content of marrow and muscle noninvasively and repeatedly within the identical volume, and it is patient-friendly (27). The multi-echo two-point DIXON-Quant (mDIXON-Quant) sequence is a three-dimensional fast-field echo (3D-FFE) sequence that uses multiple

acquired echoes to generate water, fat, and in-phase and opposed-phase images synthesized from the water-fat images. DIXON techniques are now available on the majority of clinical MRI systems with a different name (mDIXON, Philips; DIXON, Siemens; IDEAL, GE; and FatSep, Hitachi) (28). MRI using the mDIXON-Quant sequence has significant advantages over MRS, such as rapid and volumetric data acquisition with visualization of anatomical structures and quantification of fat content in a region-of-interest (ROI) (29). Multiple confounding factors including T2\* decay, T1 bias, B0 field inhomogeneity, spectral complexity of fat, noise bias, and eddy currents were presently minimized with improvements of the technique (30, 31). T2\* correction is the critical pre-step for quantitative water-fat imaging, and helps to predict the correct diagnosis of fat content in muscle and marrow (26). T1-bias effects were minimized by using a small flip angle excitation (30). Multiecho chemical shift-based water-fat separation methods have the ability to estimate and correct for field inhomogeneities using phase-correction algorithms (32), and the six peaks fat spectrum to model the spectral complexity of fat (33).

Since there is nearly no restriction on the echo times, mDIXON-Quant is different from other magnetic resonance fat quantification techniques. Full flexibility is provided by the sequence in selecting other parameters, such as scan time, resolution and field of view. The combination of fat fraction, T2\*, R2\*, water, in-phase, opposed phase images helps the radiologist for diagnosis. Tissue fat content measurement by MRI mDIXON-Quant is more efficient and accurate in a single sequence (34). However, only a few studies have attempted to measure fat content in the lumbar vertebral marrow and paraspinal muscles. This study aimed to assess the reliability of fat content measurement in lumbar vertebral marrow and paraspinal muscles utilizing MRI mDIXON-Quant.

## Methods

### Study design and participants

The calculation of sample size was based on the following criteria: 1) intraclass correlation coefficients ( $ICC_{intra}$ ) or interclass correlation coefficients ( $ICC_{inter}$ ) of less than 0.75 indicating poor agreement and an  $ICC_{intra}$  or  $ICC_{inter}$  greater than 0.9 indicated good agreement; 2) the number of obser-

vations per each healthy volunteer was 2; and 3) the target value was 0.80 and the confidence interval (CI) was 95%. The estimated minimum sample size required for analyzing agreement was 31 participants, based on Bonett's approximation (35).

Criteria for inclusion were age >18 years, no systemic inflammatory disease, no prior spine surgery, no scoliosis. Exclusion criteria were a general contraindication for MRI, prior spine surgery, presence of neurologic disorders, acute trauma, disorders of the spine, and systemic inflammatory disease.

The regional ethics committee approved the study and all participants provided informed consent (decision number: 201512-02).

### mDIXON-Quant examinations and measurement

All volunteers underwent lumbar MRI mDIXON-quant on a 3.0 T scanner (Ingenia, Philips Healthcare) by one observer (X.C.) The second observer (G.G.) repeated the same examination within 2 weeks. Both observers had 15 years of experience. The mDIXON sequence is a 3D-FFE sequence, and uses multiple acquired echoes to generate water, fat, T2\*, R2\*, and in-phase and opposed-phase images synthesized from the water-fat images. The scan parameters of the single breath-hold mDIXON-Quant were as follows: repetition time, 9.1 ms; echo time 1, 1.33 Vms; 6 echoes with delta echo time, 1.3 ms; field of view, 180×140×90

**Table 1.** Characteristics of the study participants (n=31)

	Mean±SD	Range
Age (y)	30.7±8.5	22–53
Weight (kg)	64.5±10.3	47–95
Height (cm)	167.8±7.3	153–185
BMI (kg/m <sup>2</sup> )	22.8±2.6	17.36–29.05
WC (cm)	82.4±7.3	68–99
HC (cm)	95.5±6	84–111
L3 FF (%)	35.05±11.02	19.87–64.96
PS FF (%)	3.46±1.28	0.56–6.21
ES FF (%)	5.32±3.55	1.12–18.85
MF FF (%)	5.39±3.29	1.44–19.38

SD, standard deviation; BMI, body mass index; WC, waist circumference; HC, hip circumference; L3, the third lumbar vertebra; FF, fat fraction; PS, psoas major muscle; ES, erector spinae; MF, multifidus muscle.

### Main points

- An excess infiltration of fat inside skeletal muscles and vertebral marrow may occur with aging and is associated with several diseases such as impaired glucose tolerance, type II diabetes, obesity, inactivity, fractures, osteoporosis, alcoholism, bed rest, starvation and myopathy.
- MRI and MRS can directly and noninvasively assess the amount of fat content in muscle and bone marrow, providing information about their structure, architecture, and metabolism.
- mDIXON-Quant sequence may represent a useful tool to assess the risk of fat infiltration related to several diseases in clinical practice.

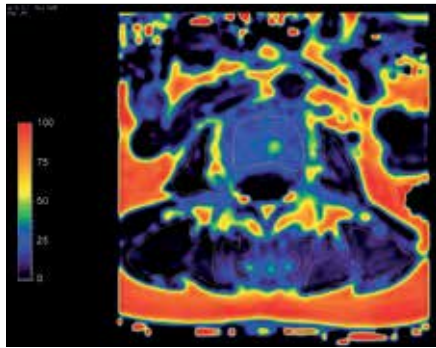


**Figure 1.** Central L3 axial magnetic resonance image shows sample regions of interest that were used to calculate the fat content of the L3 marrow and the psoas, erector spinae, and multifidus muscles.

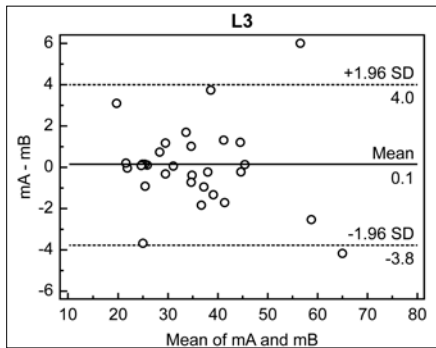


**Figure 2.** Reproducibility of L3 fat content measurements between observer A and observer B. The Bland-Altman plot shows the average values and the differences in values between observer A and observer B. The differences between the assessments of the observers do not vary in any systematic way over the measurement range. mA, mean assessment of observer A; mB, mean assessment of observer B; SD, standard deviation.

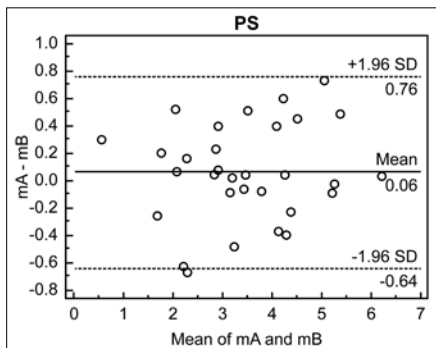


**Figure 3.** Reproducibility of the psoas major muscle fat content measurements between observer A and observer B. The Bland-Altman plot shows the average values and the differences in values between observer A and observer B. The differences between the assessments of observer A and observer B do not vary in any systematic way over the measurement range. mA, mean assessment of observer A; mB, mean assessment of observer B; PS, psoas muscle; SD, standard deviation.

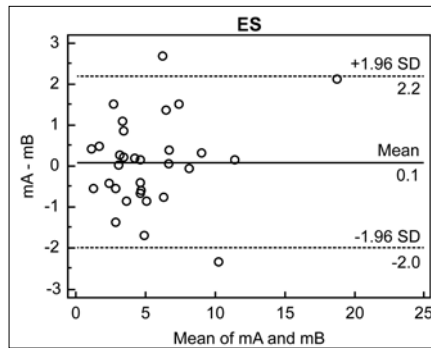


**Figure 4.** Reproducibility of the erector spinae fat content measurements between observer A and observer B. The Bland-Altman plot shows the average values and the differences in values between observer A and observer B. The differences between the assessments of observer A and observer B do not vary in any systematic way over the measurement range. mA, mean assessment of observer A; mB, mean assessment of observer B; ES, erector spinae; SD, standard deviation.

mm; flip angle, 3°; resolution, 2.5×2.5×3.0 mm; sensitivity encoding, 2; number of signal averages, 2; and scan time, 12.5 s. ROIs were drawn manually on using an ISP V7 workstation (Philips Healthcare). ROIs were drawn encompassing the largest region of the cancellous bone of vertebral bodies on central L3 axial image eliminating the vertebral cortex, Schmorl's nodules or hemangiomas (Fig. 1). The fat content of the psoas (PS), erector spinae (ES), and multifidus (MF) muscles was measured on the same central L3 axial image (Fig. 1). Clear cavities of fat at the periphery of the muscle area visually identify the edge of the muscle. Multichannel images were output by the MRI mDIXON-Quant sequence, highlighting water and fat in separate channels. We mainly use fat images to measure fat content, and different combination of images in the multichannel data could be applied to identify specific ROIs. Each observer independently measured these data, and after 2 weeks they independently remeasured the data while blinded to their previous results.

#### Statistical analysis

Reliability was assessed based on the repeatability of the intraobserver agreement between the two measurements made by the same observer. The reproducibility of the interobserver agreement was assessed by the measurements of the two observers for each volunteer. ICC<sub>intra</sub> or ICC<sub>inter</sub> with 95% CI, and the Bland-Altman method were utilized to confirm the reliability of the mDIXON-Quant method in assessing

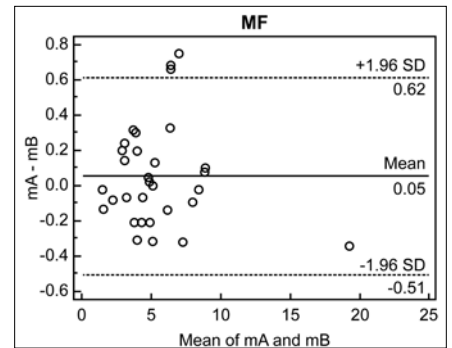


**Figure 5.** Reproducibility of the multifidus muscle fat content measurements between observer A and observer B. The Bland-Altman plot shows the average values and the differences in values between observer A and observer B. The differences between the assessments of observer A and observer B do not vary in any systematic way over the measurement range. mA, mean assessment of observer A; mB, mean assessment of observer B; MF, multifidus muscle; SD, standard deviation.

fat content in the lumbar vertebral marrow and the lumbar paraspinal muscles. An ICC<sub>intra</sub>/ICC<sub>inter</sub> less than 0.75 indicated poor agreement; an ICC<sub>intra</sub>/ICC<sub>inter</sub> in the range of 0.75–0.9 indicated moderate agreement; and an ICC<sub>intra</sub>/ICC<sub>inter</sub> above 0.9 indicated high agreement (36). Raw data were used to evaluate repeatability. The average results of the two measurements by each observer were utilized to evaluate reproducibility (i.e., interobserver agreement).

Statistical analysis was executed utilizing SPSS for Windows, version 20.0 (IBM Corp.). A statistical difference level of  $\alpha = 0.05$  was used throughout.

## Results

The participants were 15 men and 16 women with a mean age of 30.74±8.46 years (range, 22–53 years). The participants' basic characteristics and fat content results of L3 and paraspinal muscles were summarized in Table 1. The mean fat fraction of L3, PS, ES, and MF were 38.19%, 3.48%, 3.53%, respectively, for men, and 32.11%, 3.40%, 7.06%, and 7.14%, respectively, for women.

Intraobserver agreement with the mDIXON-Quant MRI was estimated using all of the original assessments of the 31 volunteers. As demonstrated in Table 2, the repeatability of the assessment of fat content in L3, PS, ES, and MF was high, and the ICC<sub>intra</sub> of the fat content were 0.997, 0.984, 0.997, and 0.995, respectively, for observer A and 0.948, 0.974, 0.963, and 0.995, respectively,

**Table 2.** Repeatability of L3 and paraspinal muscle fat fraction measurement with mDIXON imaging

Repeatability	Mean difference (%)	LoA		ICC <sub>intra</sub>	95% CI	
		Lower (%)	Upper (%)		Lower	Upper
L3 FF A1A2	-0.307	-0.625	0.010	0.997	0.993	0.998
L3 FF B1B2	-0.276	-1.628	1.077	0.948	0.897	0.975
PS FF A1A2	-0.061	-0.183	0.062	0.984	0.967	0.992
PS FF B1B2	-0.167	-0.307	-0.026	0.974	0.946	0.987
ES FF A1A2	-0.011	-0.173	-0.151	0.997	0.993	0.998
ES FF B1B2	-0.486	-0.950	-0.022	0.963	0.924	0.982
MF FF A1A2	-0.196	-0.343	-0.049	0.995	0.991	0.998
MF FF B1B2	-0.118	-0.291	0.054	0.995	0.989	0.997

L3, the third lumbar vertebra; mDIXON, multi-echo two-point Dixon sequence; LoA, limits of agreement; ICC<sub>intra</sub>, intraclass correlation coefficient; CI, confidence interval; FF, fat fraction; A1, first assessment of observer A; A2, second assessment of observer A; B1, first assessment of observer B; B2, second assessment of observer B; PS, psoas major muscle; ES, erector spinae; MF, multifidus muscle.

**Table 3.** Reproducibility of L3 and paraspinal muscle fat fraction measurement with mDIXON imaging

Reproducibility	Mean difference (%)	LoA		ICC <sub>inter</sub>	95% CI	
		Lower (%)	Upper (%)		Lower	Upper
L3 FF mA mB	0.107	-0.617	0.830	0.984	0.967	0.992
PS FF mA mB	0.062	-0.068	0.193	0.981	0.960	0.991
ES FF mA mB	0.093	-0.300	0.486	0.977	0.953	0.989
MF FF mA mB	0.054	-0.051	0.159	0.998	0.996	0.999

L3, the third lumbar vertebra; mDIXON, multi-echo two-point Dixon sequence; LoA, limits of agreement; ICC<sub>inter</sub>, interclass correlation coefficient; CI, confidence interval; FF, fat fraction; mA, mean assessment of observer A; mB, mean assessment of observer B; PS, psoas major muscle; ES, erector spinae; MF, multifidus muscle.

for observer B (Table 2). The outcomes of the Bland-Altman plots and the ICC<sub>intra</sub> were similar. The difference between the two assessments for L3, PS, ES, and MF for each observer did not vary in any systematic way over the range of measurement.

The reproducibility of the assessment of fat content in L3, PS, ES, and MF was high, and the ICC<sub>inter</sub> of the fat content was 0.984 (95% CI, 0.967–0.992), 0.981 (95% CI, 0.960–0.991), 0.977 (95% CI, 0.953–0.989), and 0.998 (95% CI, 0.996–0.999), respectively (Table 3). The outcomes of the Bland-Altman plots and the ICC<sub>inter</sub> were similar. Bland-Altman analysis according to individual reader showed only very slight mean biases (L3, 0.1%; PS, 0.06%; ES, 0.1%; MF, 0.05%) (Figs. 2–5). The difference (L3, 0.107%; PS, 0.062%; ES, 0.093%; MF, 0.054%) between the two assessments for L3, PS, ES, and MF of each

observer did not vary in any systematic way over the measurement's range (Table 3).

## Discussion

Muscular fat plays a significant role in the metabolic state of skeletal muscle and in metabolic disorders, such as type 2 diabetes, and is associated with high-intensity pain, low back pain, structural abnormality, and disability in the lumbar spine (37). The biochemical and physiological roles of the intramuscular adipose tissue are not fully known. However, this unique fat deposition may have a similar function as visceral adipose tissue in terms of the risks of metabolic impairments, such as type 2 diabetes, and it may be an index of muscular dystrophy progression (23). And bone marrow fat plays an important role in bone loss. Consequently, accurate and noninvasive measurement of

the fat content of the marrow and skeletal muscles is necessary for both exact detection of disease and exact grading of disease severity.

In this study, the reliability of fat content assessment in the lumbar vertebral marrow and the lumbar paraspinal muscles was evaluated using the mDIXON-Quant sequence. Our data demonstrated that measuring the fat content in the lumbar vertebral marrow and in the lumbar paraspinal muscles by utilizing the mDIXON-Quant sequence is highly reliable, repeatable, and reproducible. This factor ensures reliable data collection in epidemiologic surveys and in clinical practice when assessing muscle quality by monitoring morphologic changes, such as muscular atrophy and fatty infiltration. In this study, all ICC<sub>intra</sub> and ICC<sub>inter</sub> values were greater than 0.9.

Baum et al. (38) recently reported that the fat content of L1–L5 was 38.8%±7.6% in males and 31.5%±12.4% in females. L3 marrow fat content in our study was 35.05%±11.02%, which is consistent with their results. The fat content in the bone marrow usually increases with age. In other studies, the marrow fat was 60.4%±10.1% in L1–L4 (83 postmenopausal women, aged 62.8±6.6 years) (39), 56.9%±7.0% in L1–L4 (58 postmenopausal females, age range 49.2–77.4 years) (40). In another study, we measured lumbar vertebral bone marrow fat content in males as 34.1%±8.4% for 21–30 years up to 46.2%±7.4% for 61–70 years, and in females as 29.7%±7.1% for 21–30 years up to 52.5%±8.2% for 61–70 years (41). In this study, the fat contents of PS, ES, and MF were 3.52%, 3.48%, and 3.53% for men and 3.40%, 7.06%, and 7.14% for women, respectively. In the study of Fischer et al. (42), the fat content of the gastrocnemius muscle was 3.6%±4.7% in volunteers, and excellent linear correlation was shown for DIXON with phantoms and with MRS in patients. The mean fat percentage was 6%±1.6% for the nonaffected triceps brachii in the study of Duijnsveld et al. (10). Mengiardi et al. (43) reported the mean percentage fat content of the multifidus muscle as 14.5% (95% CI: 10.8%, 18.3%) in the volunteers.

The MRI mDIXON-Quant technique has been widely utilized in other literatures to quantify hepatic steatosis and is increasingly utilized to quantify intramuscular fat (44–47) and bone marrow fat. The mDIXON-Quant imaging technique permits a more rapid and accurate assessment of the fat content of tis-

sue in a single sequence (34). This approach permits confirmation of the fat-to-water ratio and correction of T2\* effects without the necessity for extra sequences to address mapping and potential misregistration of the image (34). The multiecho chemical shift-based water-fat separation techniques has been shown to be in good one-to-one agreement with the chemically calculated fat fraction *in vitro* in water-fat bone phantoms ( $R^2=0.97$ ) and with the MRS-based fat fraction *in vivo* in the bone marrow of the proximal femur ( $R^2=0.87$ ) and lumbar vertebrae ( $R^2=0.959$ ) (33, 39, 48). The study of Lee et al. (49) also show that fat fraction of phantoms measured with mDIXON MRI was strongly correlated with actual fat content of lumbar vertebrae ( $P < 0.01$ ,  $R^2 = 0.93$ ). One study (42) demonstrated that mDIXON-Quant imaging allows accurate measurement of muscle fat content in a phantom as well as in patients and healthy volunteers. In that study, the *in vivo* results of mDIXON-Quant and MRS were closely and significantly matched. Another study (28) compared different DIXON-based fat quantification methods using MRS as the standard of reference, and found that mDIXON-Quant imaging had good linearity and low variability when used to quantify intramuscular fat; a low flip angle was suggested to be used to reduce T1 effects. Compared with MRS, *in vitro* in fat-water phantoms, all mDIXON sequences correlated significantly with MRS ( $r > 0.97$ ,  $P < 0.002$ ) (28).

The mDIXON-Quant imaging technique potentially has significant advantages over MRS, such as fast volumetric coverage of the muscular anatomy, with the potential for postprocessing, such as multiplanar reformation (50). In addition, mDIXON-Quant imaging can obtain R2\* mapping, which has multiple applications in MRI, such as for detecting superparamagnetic iron oxide, assessing blood oxygenation, and evaluating tissue iron levels (51). The study of Serai et al. (52) shows that hepatic fat fraction measurement by utilizing mDIXON Quant and IDEAL IQ can be highly reproduced across imaging platforms, readers, and field strengths, with only minimal average bias that is probably clinically irrelevant in most cases. The potential causes of differences between two techniques include incompletely corrected T1 bias, technical differences, and calculation differences (52).

The paraspinal muscle cross-section area is largest overall at the L3–L4 level (53). Therefore, we chose to measure the fat content in the lumbar vertebral marrow

and lumbar paraspinal muscle on central L3 axial images. Analysis of the fat content was performed through ROI analysis. In the present study, we selected an anatomical approach and included the entire muscle in the ROI, based on the muscular compartment's outline.

One limitation of this study was that there was no histologic determination, especially of the fat content distribution in each individual. However, biopsy is an invasive procedure, and is associated with a substantial degree of sampling error and complications, such as pain. Based on the above reasons, we did not perform biopsies for quantification of fat content. A second limitation is that the borders and position of the ROIs between each examination were not identical, which may lead to error in measurements. Finally, only 31 people were included. Larger sample sizes are certainly needed.

In conclusion, the repeatability and reproducibility of fat content measurement in the lumbar vertebral marrow and lumbar paraspinal muscles utilizing mDIXON-Quant sequence were high. This technique may provide a new and easier approach for lumbar vertebral marrow and lumbar paraspinal muscle fat content quantification, and it could help explore risks associated with diseases such as osteoporosis and diabetes.

#### Conflict of interest disclosure

The authors declared no conflicts of interest.

#### Research Funding

This work was supported by Beijing Municipal Bureau of Health of 215 program [grant number 2009-02-03]; and Capital Health Research and Development of Special [grant number 2014-2-1122]. The funding agencies had no role in the study design, the collection, analysis, or interpretation of data, the writing of the report, or the decision to submit the article for publication.

#### References

- Schrauwenhinderling VB, Hesselink MK, Schrauwen P, Kooi ME. Intramyocellular lipid content in human skeletal muscle. *Obesity* 2012; 14:357–367. [CrossRef]
- Aubrey J, Esfandiari N, Baracos VE, et al. Measurement of skeletal muscle radiation attenuation and basis of its biological variation. *Acta Physiol (Oxf)* 2014; 210:489–497. [CrossRef]
- Wronska A, Kmiec Z. Structural and biochemical characteristics of various white adipose tissue depots. *Acta Physiol (Oxf)* 2012; 205:194–208. [CrossRef]

- Saukkonen T, Heikkinen S, Hakkarainen A, et al. Association of intramyocellular, intraperitoneal and liver fat with glucose tolerance in severely obese adolescents. *Eur J Endocrinol* 2010; 163:413–419. [CrossRef]
- Schafer AL, Vittinghoff E, Lang TF, et al. Fat infiltration of muscle, diabetes, and clinical fracture risk in older adults. *J Clin Endocr Metab* 2010; 95:368–372. [CrossRef]
- Goodpaster BH, Thaete FL, Kelley DE. Thigh adipose tissue distribution is associated with insulin resistance in obesity and in type 2 diabetes mellitus. *Am J Clin Nutr* 2000; 71:885–892. [CrossRef]
- Taaffe DR, Henwood TR, Nalls MA, Walker DG, Lang TF, Harris TB. Alterations in muscle attenuation following detraining and retraining in resistance-trained older adults. *Gerontology* 2009; 55:217–223. [CrossRef]
- Murphy RA, Mourtzakis M, Chu QS, Baracos VE, Reiman T, Mazurak VC. Nutritional intervention with fish oil provides a benefit over standard of care for weight and skeletal muscle mass in patients with nonsmall cell lung cancer receiving chemotherapy. *Cancer* 2011; 117:1775–1782. [CrossRef]
- Paalanne N, Niinimäki J, Karppinen J, et al. Assessment of association between low back pain and paraspinal muscle atrophy using opposed-phase magnetic resonance imaging: a population-based study among young adults. *Spine (Phila Pa 1976)* 2011; 36:1961–1968. [CrossRef]
- Duijnsveld BJ, Henseler JF, Reijnierse M, Fiocco M, Kan HE, Nelissen RG. Quantitative Dixon MRI sequences to relate muscle atrophy and fatty degeneration with range of motion and muscle force in brachial plexus injury. *Magn Reson Imaging* 2017; 36:98–104. [CrossRef]
- Akima H, Hioki M, Furukawa T. Effect of arthroscopic partial meniscectomy on the function of quadriceps femoris. *Knee Surg Sports Traumatol Arthrosc* 2008; 16:1017–1025. [CrossRef]
- Manini TM, Clark BC, Nalls MA, Goodpaster BH, Ploutznyder LL, Harris TB. Reduced physical activity increases intermuscular adipose tissue in healthy young adults. *Am J Clin Nutr* 2007; 85:377–384. [CrossRef]
- Lithell H, Orlander J, Schéle R, Sjödin B, Karlsson J. Changes in lipoprotein-lipase activity and lipid stores in human skeletal muscle with prolonged heavy exercise. *Acta Physiol Scand* 1979; 107:257–261. [CrossRef]
- Griffith JF, Yeung DK, Antonio GE, et al. Vertebral bone mineral density, marrow perfusion, and fat content in healthy men and men with osteoporosis: dynamic contrast-enhanced MR imaging and MR spectroscopy. *Radiology* 2005; 236:945–951. [CrossRef]
- Chen WT, Shih TT, Chen RC, et al. Vertebral bone marrow perfusion evaluated with dynamic contrast-enhanced MR imaging: significance of aging and sex. *Radiology* 2001; 220:213–218. [CrossRef]
- Maurel DB, Boisseau N, Benhamou CL, Jaffre C. Alcohol and bone: review of dose effects and mechanisms. *Osteoporosis Int* 2012; 23:1–16. [CrossRef]

17. Ecklund K, Vajapeyam S, Feldman HA, et al. Bone marrow changes in adolescent girls with anorexia nervosa. *J Bone Miner Res* 2010; 25:298–304. [\[CrossRef\]](#)
18. Trudel G, Payne M, Madler B, et al. Bone marrow fat accumulation after 60 days of bed rest persisted 1 year after activities were resumed along with hemopoietic stimulation: the Women International Space Simulation for Exploration study. *J Appl Physiol* (1985) 2009; 107:540–548. [\[CrossRef\]](#)
19. Minaire P, Edouard C, Arlot M, Meunier PJ. Marrow changes in paraplegic patients. *Calcif Tissue Int* 1984; 36:338–340. [\[CrossRef\]](#)
20. Templeton ZS, Lie WR, Wang W, et al. Breast cancer cell colonization of the human bone marrow adipose tissue niche. *Neoplasia* 2015; 17:849–861. [\[CrossRef\]](#)
21. Johnell O, Kanis J. Epidemiology of osteoporotic fractures. *Horm Res* 2006; 54:1–13.
22. Fischer MA, Nanz D, Shimakawa A, et al. Quantification of muscle fat in patients with low back pain: comparison of multi-echo MR imaging with single-voxel MR spectroscopy. *Radiology* 2013; 266:555–563. [\[CrossRef\]](#)
23. Akima H, Hioki M, Yoshiko A, et al. Intramuscular adipose tissue determined by T1-weighted MRI at 3T primarily reflects extramyocellular lipids. *Magn Reson Imaging* 2016; 34:397–403. [\[CrossRef\]](#)
24. Arts IM, Pillen S, Schelhaas HJ, Overeem S, Zwartz MJ. Normal values for quantitative muscle ultrasonography in adults. *Muscle Nerve* 2010; 41:32–41. [\[CrossRef\]](#)
25. Strauss S, Gavish E, Gottlieb P, Katsnelson L. Interobserver and intraobserver variability in the sonographic assessment of fatty liver. *AJR Am J Roentgenol* 2007; 189:W320–323. [\[CrossRef\]](#)
26. Schwenzer NF, Martirosian P, Machann J, et al. Aging effects on human calf muscle properties assessed by MRI at 3 Tesla. *J Magn Reson Imaging* 2010; 29:1346–1354. [\[CrossRef\]](#)
27. Mehta SR, Thomas EL, Bell JD, Johnston DG, Taylor-Robinson SD. Non-invasive means of measuring hepatic fat content. *World J Gastroenterol* 2008; 14:3476–3483. [\[CrossRef\]](#)
28. Noble JJ, Keevil SF, Totman J, Charles-Edwards GD. In vitro and in vivo comparison of two-, three- and four-point Dixon techniques for clinical intramuscular fat quantification at 3 T. *Brit J Radiol* 2014; 87:20130761. [\[CrossRef\]](#)
29. Rofsky NM, Lee VS, Laub G, et al. Abdominal MR imaging with a volumetric interpolated breath-hold examination. *Radiology* 1999; 212:876–884. [\[CrossRef\]](#)
30. Yang IY, Cui Y, Wiens CN, Wade TP, Friesen-Waldner LJ, Mckenzie CA. Fat fraction bias correction using T1 estimates and flip angle mapping. *J Magn Reson Imaging* 2013; 39:217–223. [\[CrossRef\]](#)
31. Karampinos DC, Ruschke S, Dieckmeyer M, et al. Modeling of T2\* decay in vertebral bone marrow fat quantification. *Nmr Biomed* 2015; 28:1535–1542. [\[CrossRef\]](#)
32. Yu H, Shimakawa A, Mckenzie CA, Brodsky E, Brittain JH, Reeder SB. Multiecho water-fat separation and simultaneous R2\* estimation with multifrequency fat spectrum modeling. *Magn Reson Med* 2008; 60:1122–1134. [\[CrossRef\]](#)
33. Gee CS, Nguyen JT, Marquez CJ, et al. Validation of bone marrow fat quantification in the presence of trabecular bone using MRI. *J Magn Reson Imaging* 2015; 42:539–544. [\[CrossRef\]](#)
34. O'Regan DP, Callaghan MF, Wylezinskaaridge M, et al. Liver fat content and T2\*: simultaneous measurement by using breath-hold multiecho MR imaging at 3.0T-feasibility. *Radiology* 2008; 247:550–557. [\[CrossRef\]](#)
35. Bonett DG. Sample size requirements for estimating intraclass correlations with desired precision. *Stat Med* 2002; 21:1331–1335. [\[CrossRef\]](#)
36. McGraw KO, Wong SP. Forming inferences about some intraclass correlation coefficients. *Psychol Methods* 1996; 1:30–46. [\[CrossRef\]](#)
37. Teichtahl AJ, Urquhart DM, Wang Y, et al. Fat infiltration of paraspinal muscles is associated with low back pain, disability, and structural abnormalities in community-based adults. *Spine J* 2015; 15:1593–1601. [\[CrossRef\]](#)
38. Baum T, Yap SP, Dieckmeyer M, et al. Assessment of whole spine vertebral bone marrow fat using chemical shift-encoding based water-fat MRI. *J Magn Reson Imaging* 2015; 42:1018–1023. [\[CrossRef\]](#)
39. Li G, Xu Z, Gu H, et al. Comparison of chemical shift-encoded water-fat MRI and MR spectroscopy in quantification of marrow fat in postmenopausal females. *J Magn Reson Imaging* 2016; 45:66–73. [\[CrossRef\]](#)
40. Li GW, Xu Z, Chen QW, et al. Quantitative evaluation of vertebral marrow adipose tissue in postmenopausal female using MRI chemical shift-based water-fat separation. *Clin Radiol* 2014; 69:254–262. [\[CrossRef\]](#)
41. Zhang y, Cheng XG, Yu Al'H, et al. Quantitative radiological evaluation of interaction of lumbar vertebral bone marrow fat, bone mineral density and age. *Zhonghua Fang She Xue Za Zhi* 2017; 51:771–776.
42. Fischer MA, Pfirrmann CW, Espinosa N, Raptis DA, Buck FM. Dixon-based MRI for assessment of muscle-fat content in phantoms, healthy volunteers and patients with achillodynia: comparison to visual assessment of calf muscle quality. *Eur Radiol* 2014; 24:1366–1375. [\[CrossRef\]](#)
43. Mengiardi B, Schmid MR, Boos N, et al. Fat content of lumbar paraspinal muscles in patients with chronic low back pain and in asymptomatic volunteers: quantification with MR spectroscopy. *Radiology* 2006; 240:786–792. [\[CrossRef\]](#)
44. Wokke BH, Bos C, Reijnierse M, et al. Comparison of dixon and T1-weighted MR methods to assess the degree of fat infiltration in duchenne muscular dystrophy patients. *J Magn Reson Imaging* 2013; 38:619–624. [\[CrossRef\]](#)
45. Reeder SB, Sirlin CB. Quantification of liver fat with magnetic resonance imaging. *Magn Reson Imaging Clin N Am* 2010; 18:337–357. [\[CrossRef\]](#)
46. Fischmann A, Faslser S, Gloor M, Bieri O, Studler U, Fischer D. Quantitative MRI can detect subclinical disease progression in muscular dystrophy. *J Neurol* 2012; 259:1648–1654. [\[CrossRef\]](#)
47. Wren TA, Bluml S, Tsengong L, Gilsanz V. Three-point technique of fat quantification of muscle tissue as a marker of disease progression in Duchenne muscular dystrophy: preliminary study. *AJR Am J Roentgenol* 2008; 190:8–12. [\[CrossRef\]](#)
48. Karampinos DC, Melkus G, Baum T, Bauer JS, Rummeny EJ, Krug R. Bone marrow fat quantification in the presence of trabecular bone: Initial comparison between water-fat imaging and single-voxel MRS. *Magn Reson Med* 2014; 71:1158–1165. [\[CrossRef\]](#)
49. Lee SH, Lee YH, Hahn S, Suh JS. Fat fraction estimation of morphologically normal lumbar vertebrae using the two-point mDixon turbo spin-echo MRI with flexible echo times and multipeak spectral model of fat: Comparison between cancer and non-cancer patients. *Magn Reson Imaging* 2016; 34:1114–1120. [\[CrossRef\]](#)
50. Ma J. Dixon techniques for water and fat imaging. *J Magn Reson Imaging* 2008; 28:543–558. [\[CrossRef\]](#)
51. Hernando D, Kuhn JP, Mensel B, et al. R2\* estimation using “in-phase” echoes in the presence of fat: The effects of complex spectrum of fat. *J Magn Reson Imaging* 2013; 37:717–726. [\[CrossRef\]](#)
52. Serai SD, Dillman JR, Trout AT. Proton density fat fraction measurements at 1.5- and 3-T hepatic MR imaging: same-day agreement among readers and across two imager manufacturers. *Radiology* 2017; 284:244–254. [\[CrossRef\]](#)
53. Mannion AF, Taimela S, Muntener M, Dvorak J. Active therapy for chronic low back pain part 1. Effects on back muscle activation, fatigability, and strength. *Spine (Phila Pa 1976)* 2001; 26:897–908. [\[CrossRef\]](#)